Dissecting the role of sodium currents in visceral sensory neurons in a model of chronic hyperexcitability using $Na_V1.8$ and $Na_V1.9$ null mice

Kirk Hillsley[1], Jia-Hui Lin[1], Andre Stanisz[1], David Grundy[1] Jeroen Aerssens[2], Pieter J. Peeters[2], Diederik Moechars[2], Bernard Coulie[2] and Ronald H. Stead[1]

[1]*Holburn Group, Bowmanville, Ontario, Canada,* [2]*Johnson & Johnson Pharmaceutical Research and Development, Beerse, Belgium*

Tetrodotoxin-resistant (TTX-R) sodium currents have been proposed to underlie sensory neuronal hyperexcitability in acute inflammatory models, but their role in chronic models is unknown. Since no pharmacological tools to separate TTX-R currents are available, this study employs $Na_v1.8$ and $Na_v1.9$ null mice to evaluate these currents roles in a chronic hyperexcitability model after the resolution of an inflammatory insult. Transient jejunitis was induced by infection with *Nippostrongylus brasiliensis* (Nb) in $Na_v1.9$ and $Na_v1.8$ null, wild-type and naïve mice. Retrogradely labelled dorsal root ganglia (DRG) neurons were harvested on day 20–24 post-infection for patch clamp recording. Rheobase and action potential (AP) parameters were recorded as measures of excitability, and $Na_v1.9$ and $Na_v1.8$ currents were recorded. DRG neuronal excitability was significantly increased in post-infected mice compared to sham animals, despite the absence of ongoing inflammation (sham $= 1.9 \pm 0.3$, infected $= 3.6 \pm 0.7$ APs at $2\times$ rheobase, $P = 0.02$). Hyperexcitability was associated with a significantly increased amplitude of TTX-R currents. Hyperexcitability was maintained in $Na_v1.9^{-/-}$ mice, but hyperexcitability was absent and APs were blunted in $Na_v1.8^{-/-}$ mice. This study identifies a critical role for $Na_v1.8$ in chronic post-infectious visceral hyperexcitability, with no contribution from $Na_v1.9$. Nb infection-induced hyperexcitability is not observed in $Na_v1.8^{-/-}$ mice, but is still present in $Na_v1.9^{-/-}$ mice. It is not clear whether hyperexcitability is due to a change in the function of $Na_v1.8$ channels or a change in the number of $Na_v1.8$ channels.

(Resubmitted 15 May 2006; accepted after revision 17 July 2006; first published online 20 July 2006)
Corresponding author R. H. Stead: Holburn Group, 1100 Bennett Road, Bowmanville, Canada ON L1C 3K5.
Email: ronald.stead@holburn.com

Gastrointestinal (GI) infections can cause inflammation and altered intestinal function. Although acute infections are resolved quickly, GI function and sensation can remain abnormal for prolonged periods in some patients (Spiller, 2004). Various studies have investigated neuronal changes during the acute infection/inflammation period, and reported a hyperexcitability of sensory neurons innervating the GI tract. Intrinsic neurons have been found to be hyperexcitable due to alterations in the cyclooxygenase and serotonergic pathways (Linden *et al.* 2004). Models investigating acute neuronal excitability in extrinsic neurons supplying the GI tract have found changes in voltage-activated tetrodotoxin-resistant (TTX-R) sodium currents (Beyak *et al.* 2004).

TTX-R currents are expressed almost exclusively on sensory neurons of vagal, spinal, trigeminal and enteric origin, although cerebellar Purkinje cells can express functional TTX-R currents (Renganathan *et al.* 2003). There are at least two different TTX-R currents with distinct properties. There is a slowly inactivating current which is mediated by the $Na_v1.8$ channel. $Na_v1.8$ is more abundantly expressed in small-diameter dorsal root ganglion (DRG) neurons (Malik-Hall *et al.* 2003; Djouhri *et al.* 2003), but is also responsible for the slow current in large (>40 pF) DRG neurons (Renganathan *et al.* 2000). The second TTX-R current has even slower inactivation kinetics; this persistent TTX-R current is mediated by the $Na_v1.9$ channel. In myenteric sensory neurons there is no evidence for $Na_v1.8$ expression, but $Na_v1.9$ is present (Rugiero *et al.* 2003).

There have been many studies investigating the roles of $Na_v1.8$ and $Na_v1.9$. The TTX-R current that contributes to the upstroke of the action potential (AP) is almost exclusively $Na_v1.8$. In studies on $Na_v1.8^{+/+}$ and $Na_v1.8^{-/-}$ mice, most $Na_v1.8^{+/+}$ DRG neurons generate all-or-none APs, whereas most $Na_v1.8^{-/-}$ neurons exhibit smaller graded responses, with smaller peaks and slower rise times (Renganathan *et al.* 2001). This paper estimated

 DOI: 10.1113/jphysiol.2006.113597

that $Na_v1.8$ contributed 80–90% of the inward current flow during the AP upstroke. $Na_v1.8$ is also essential for spontaneous AP activity in damaged sensory neurons (Roza *et al.* 2003).

The $Na_v1.9$ current is not a major contributor to the AP upstroke in $Na_v1.8^{-/-}$ mice (Herzog *et al.* 2001). $Na_v1.9$ is proposed to play a role in setting the resting membrane potential value and modulating responses to subthreshold stimuli (Cummins *et al.* 1999; Herzog *et al.* 2001; Dib-Hajj *et al.* 1999). Peripheral axotomy results in a downregulation of $Na_v1.9$ that is modulated by glial cell-derived neurotrophic factor (GDNF) (Fjell *et al.* 1999). There is conflicting evidence from differing models on the role of $Na_v1.9$ in inflammation. Little change in $Na_v1.9$ expression has been observed during inflammation in some studies (Black *et al.* 2004; Coggeshall *et al.* 2004), whereas a recent paper showed that $Na_v1.9$ contributed to thermal hypersensitivity and spontaneous pain behaviour after peripheral inflammation (Priest *et al.* 2005). Furthermore, application of the inflammatory agent prostaglandin E_2 has recently been shown to increase $Na_v1.9$ currents via a G-protein-dependent mechanism (Rush & Waxman, 2004).

There are several studies suggesting that $Na_v1.8$ plays a critical role in acute inflammatory hyperexcitability. In inflamed hind paw models, there is an upregulation in $Na_v1.8$ expression and the slowly inactivating TTX-R current (Black *et al.* 2004), and an increase in $Na_v1.8$ immunoreactivity, especially in unmyelinated axons (Coggeshall *et al.* 2004). DRG neurons from $Na_v1.8^{-/-}$ knockout mice display weak responses, and the mice show no referred hyperalgesia to intracolonic capsaicin or mustard oil (Laird *et al.* 2002). Hyperexcitability in mice DRG with trinitro genzone sulfonic acid (TNBS)-induced colitis is associated with an increase in $Na_v1.8$ during the acute inflammation (Beyak *et al.* 2004). The same insult has also been shown to cause increased excitability in intestinal myenteric sensory neurons, but there is no evidence that this is due to changes in TTX-R currents (Linden *et al.* 2003).

It is clear that TTX-R Na_v channels can have profound influences on neuronal excitability. However, all of these studies have investigated the acute changes that occur coincidentally with the pathophysiological insult. This study utilized nematode infection with *Nippostrongylus brasiliensis* (Nb) as an insult that causes transient jejunitis (Mahida, 2003) and hypersensitivity (McLean *et al.* 1997). The primary aim of this study was to determine whether there are any longer term changes in neuronal excitability and TTX-R currents after an acute inflammatory episode has occurred in the absence of any ongoing insult. To this end, uniquely either $Na_v1.9$ or $Na_v1.8$ null mice were utilized to determine the relative importance of each channel in the observed hyperexcitability following Nb infection.

Methods

Animals

Balb/c mice (Charles River Laboratories, Quebec, Canada) were used in the study. In addition, knockout mice and their littermate controls (homozygous wild-type), generated in a mixed genetic background of C57Bl6/129SvEvBrd mice (see below), were used in follow-up experiments. Each mouse strain underwent identical infection, labelling, cell isolation and recording procedures. All protocols and surgical procedures were approved by an independent Institutional Animal Care and Use Committee, in accordance with the guidelines of the American Association for Laboratory Animal Science.

Generation of $Na_v1.8^{-/-}$ and $Na_v1.9^{-/-}$ mice

Genomic clones containing $Na_v1.8$ or $Na_v1.9$ sequences were identified by screening a 129SvEvBrd-derived lambda pKOS mouse genomic library with $Na_v1.8$ or $Na_v1.9$ sequence-specific primers. For $Na_v1.8$ an 8.5 kb genomic clone containing exons 6 to 11 was used to generate the targeting vector. Heterozygous $Na_v1.8^{+/-}$ mice were generated by Lexicon Genetics Inc. (The Woodlands, Texas) by replacing exons 8 to 10 (ENSMUST00000037936, ENSEMBL) with an IRES LacZ/MC1-Neo reporter gene/selection cassette. The structure of the targeted $Na_v1.8$ locus is shown in Fig. 1*A*. For $Na_v1.9$, a 10.5 kb genomic clone containing exons 2 and 3 (ENSMUSG00000034115, ENSEMBL) was used to generate the targeting vector. Heterozygous $Na_v1.9^{+/-}$ mice were generated by Lexicon Genetics Inc. by replacing exon 2 with an IRES LacZ/MC1-Neo reporter gene/selection cassette. The structure of the targeted $Na_v1.9$ locus is shown in Fig. 1*C*. The vectors were linearized by digestion with *Not*I, and electroporated into 129SvEvBrd (LEX1) ES cells. G418-5 fialuridine-resistant embryonic stem (ES) cell clones were isolated and verified for homologous recombination at the $Na_v1.8$ or $Na_v1.9$ locus by Southern blot analysis. ES cell clones containing the targeting construct were injected into C57BL/6(albino) blastocysts, and the resulting chimeras were mated with C57BL/6(albino) females to generate heterozygous animals harbouring a disrupted $Na_v1.8$ or $Na_v1.9$ allele. Heterozygous mice were subsequently crossed to generate mice with homogeneous genotypes employed in the present studies. Genotyping was carried out by PCR on DNA isolated from mouse tail biopsy samples. Reactions containing primer pairs 5′-GCC-ATG-CCC-AAT-CCC-ACT-ACT-G-3′ and 5′-CAA-CTG-CTG-CCA-ACC-TAG-CTT-AG-3′ ($Na_v1.8$) or 5′-GTC-TGA-GCC-AAG-GGT-GAA-G-3′ and 5′-CGT-CGC-CAT-AGA-GCT-TAG-GT-3′ ($Na_v1.9$) resulted in the

amplification of a 475 bp or 224 bp product from the wild-type allele for $Na_v1.8$ or $Na_v1.9$, respectively, while reactions using primer pair 5′-CAA-CTG-CTG-CCA-ACC-TAG-CTT-AG-3′ and 5′-GCA-GCG-CAT-CGC-CTT-CTA-TC-3′ ($Na_v1.8$) or 5′-AAC-CTT-TCA-GAG-TCA-GCC-TC-3′ and 5′-GCA-GCG-CAT-CGC-CTT-CTA-TC-3′ ($Na_v1.9$) amplified a 307 bp or 314 bp product from the disrupted allele of $Na_v1.8$ or $Na_v1.9$, respectively.

Loss of expression of the $Na_v1.8$ or $Na_v1.9$ transcript in the knockout mice was confirmed by quantitative RTq-PCR performed on total RNA, isolated from spinal cord, dorsal root ganglia and brain from wild-type and homozygote $Na_v1.8^{-/-}$ or $Na_v1.9^{-/-}$ animals. $Na_v1.8$ and $Na_v1.9$ was absent in all tissues derived from the respective homozygote knockout mice, as illustrated in Fig. 1*D* and *E*. Both $Na_v1.8^{-/-}$ and $Na_v1.9^{-/-}$ mice were born at expected Mendelian frequencies, and were indistinguishable from wild-type littermates in terms of development, growth and fertility. Assays were also performed to determine baseline immune function (haematology screen, fluorescence activated cal sorter (FACS) mononuclear cell profile, ovalbumin challenge, and lipopolysaecharide (LPS) acute phase response), metabolic function (blood chemistry screen, weight/growth curve, oral glucose test, and DEXA bone density scan) and neurological function

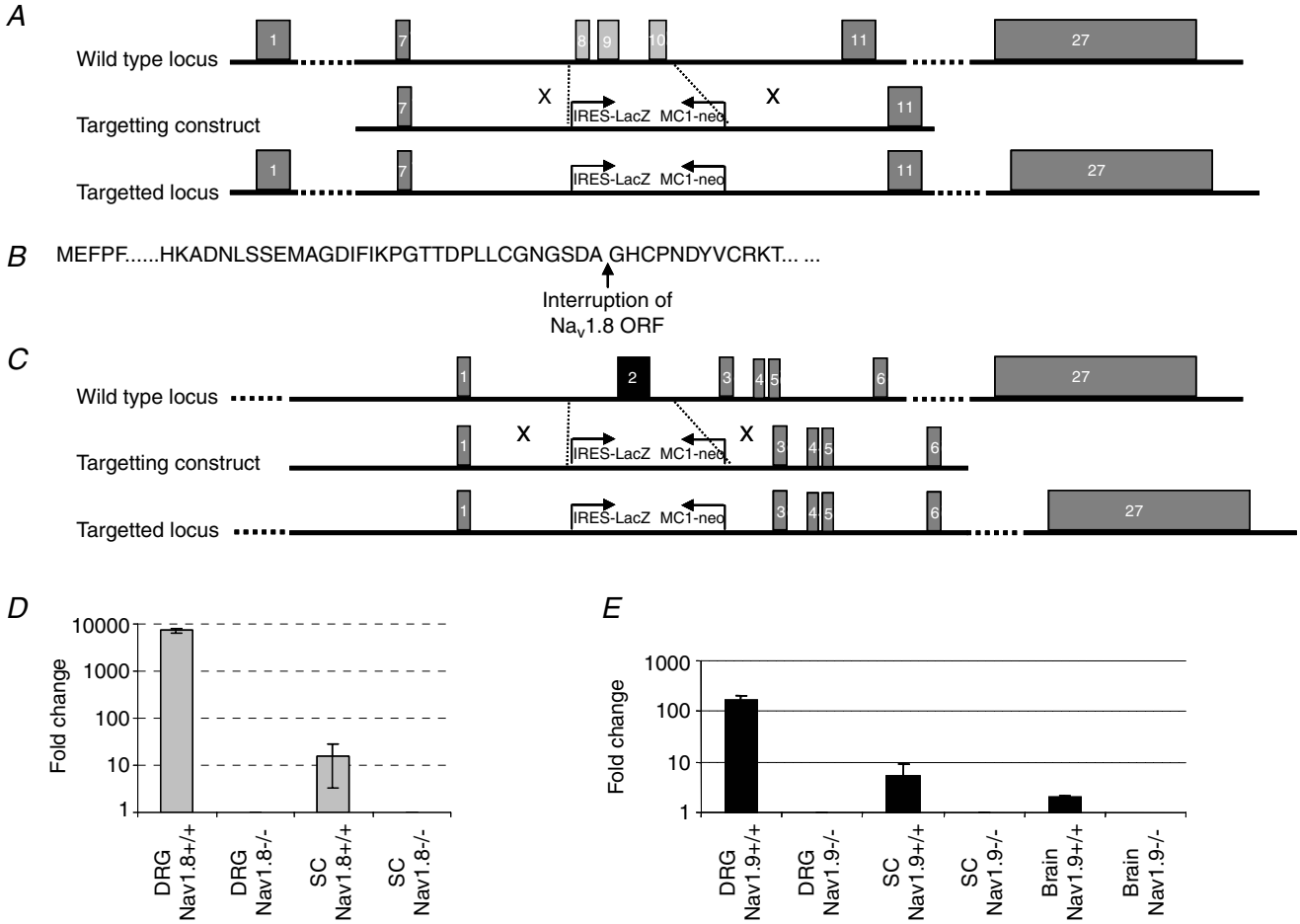

Figure 1. Targeted disruption of the $Na_v1.8$ and $Na_v1.9$ gene
A, structure of the $Na_v1.8$ wild-type locus, targeting vector and recombinant locus. Boxes represent exons. A lambda pKOS-based targeting construct was generated by replacing a gDNA fragment spanning exon 8 to exon 10 by the IRESLacZ/MC1-Neo reporter/selection cassette, disrupting the open reading frame (site of interruption shown in *B*). *C*, structure of the $Na_v1.9$ wild-type locus, targeting the vector and recombinant locus. Boxes represent exons. A lambda pKOS-based targeting construct was generated by replacing a gDNA fragment spanning the first coding exon (exon 2) by the IRESLacZ/MC1-Neo reporter/selection cassette. *D*, expression of the $Na_v1.8$ transcript in dorsal root ganglia (DRG) and spinal cord (SC) was abolished in the $Na_v1.8^{-/-}$ mouse as determined by quantitative RT-PCR. Values expressed are mean ($n = 5$) relative expression levels after normalization to β-actin. *E*, expression of the $Na_v1.9$ transcript in brain, dorsal root ganglia (DRG) and spinal cord (SC) was abolished in the $Na_v1.9^{-/-}$ mouse as determined by quantitative RT-PCR. Values expressed are mean ($n = 6$) relative expression levels after normalization to β-actin.

(open field test, inverted screen test, acoustic startle response, tail flick and hot plate test): no differences were recorded in knockout mice.

Infection

Mice were infected with *Nippostrongylus brasiliensis* (Nb). Nb L3 stage larvae were isolated, counted and visually checked for motility prior to injection. Nb larvae were suspended in a PBS solution containing penicillin (100 u ml^{-1}) and streptomycin (100 $\mu g\,ml^{-1}$). Sham animals were given a subcutaneous injection (0.2 ml) of PBS/penicillin/streptomycin solution. Infected animals were given 500 L3 Nb larvae in this solution. At the time of experimentation (19–25 days post-Nb infection) there was no indication of inflammation or oedema in any animal as shown in Fig. 2, consistent with prior studies in the mouse (Stadnyk *et al.* 1990).

Neuronal preparation

16–20 days post-Nb infection, mice were injected intraperitoneally with 100 μl cholera toxin subunit-B with a 488-nm fluorescent tag (CTB-488, Molecular Probes, OR, USA). This labelling methodology has previously been documented (Peeters *et al.* 2006) and applied as an alternative to intramuscular injection into GI smooth muscle, which is complicated by the accompanying surgery necessary. Intraperitoneal injection labels more neurons than intramuscular injection, but it enriches for DRG neurons projecting to the peritoneal cavity, with the majority (>90%) of labelled neurons occurring between T9 and T13, similar to the distribution of labelled neurons after intramuscular injection into GI smooth muscle (Peeters *et al.* 2006). Intraperitoneal labelling has previously been shown to be a reliable method for labelling neurons supplying the abdominal cavity (Anderson & Edwards, 1994; Leong & Ling, 1990).

Three to five days later, mice were killed by an overdose of anaesthetic (ketamine and xylazine i.p., 160 and 100 mg kg^{-1}, respectively). DRG from T9–T13 were removed, and dissociated by mechanical and chemical disruption. After breaking DRG apart mechanically, the partially dissociated ganglia were incubated at 37°C in collagenase type I (2 mg ml^{-1}) for 45 min and 0.25% trypsin for a further 35 min. After deactivation with 10% fetal calf serum, cells were plated on poly D-lysine-coated culture dishes and cultured overnight in L-15 media prior to patch-clamp recordings.

Electrophysiological recordings

Recordings were only made from fluorescent neurons. Cell fluorescence was checked using a Leica inverted microscope (DMIRE2, Leica, Canada) equipped with fluorescent filters to detect CTB-488. Whole-cell currents and voltage-clamp experiments were performed by using a MultiClamp 7A amplifier, and digitized with a DigiData 1322A converter (Axon Instruments). Stimulation and data acquisition were carried out by pClamp 9 programs (Axon Instruments). Signals were sampled at 10 kHz or 20 kHz, and low-pass filtered at 4 KHz. The series resistance was compensated as much as possible. Neurons were excluded from analysis if the seal resistance or access resistance was unstable.

Borosilicate glass (Harvard) was pulled with a P97 micropipette puller (Sutter, CA, USA), and fire polished by a MF 200 microforge (World Precision Instrument) to a tip resistance of 5–10 MΩ. A silver–silver chloride pellet (World Precision Instrument) was placed in the recording dish as the reference electrode. The normal extracellular Krebs solution contained (mM): NaCl 118.0, KCl 4.7, NaH_2PO_4 1.0, $NaHCO_3$ 25.0, $MgSO_4$ 1.2, $CaCl_2$ 2.5, D-glucose 11.1, with pH adjusted to 7.3 by using NaOH. The normal intracellular solution contained (mM): Hepes 10.0, KCl 130.0, $MgCl_2$ 1.0, $CaCl_2$ 1.0, EGTA 2.0, K_2ATP 2, Na_3GTP 0.2, titrated with KOH to pH 7.25. The extracellular solution for isolating TTX-resistant Na^+ currents was composed of (mM): NaCl 145.0, KCl 4.8, Hepes 10.0, $MgCl_2$ 1.0, $CaCl_2$ 2.5, D-glucose 11.1, TTX 0.0003, CdCl 0.5, 4-AP 1.0, TEA-Cl 5.0, CsCl 2.0,

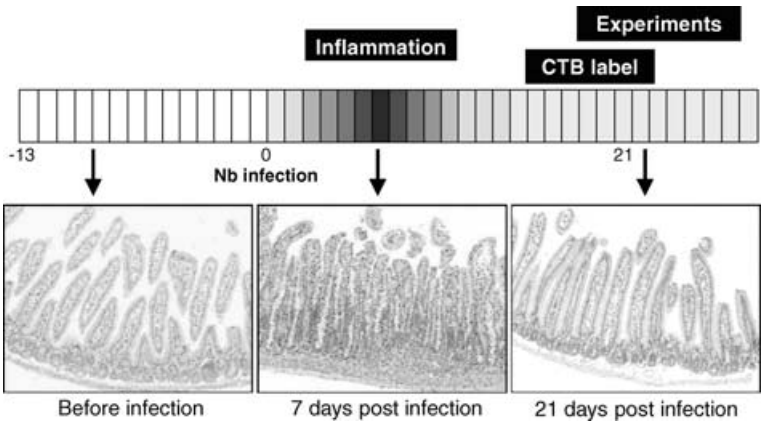

Figure 2. Experimental time course schematic illustrating the effect of Nb infection on jejunal histology
Each image shows a typical haematoxylin and eosin-stained jejunal section at different time points throughout the experiment. Prior to exposure to Nb, the jejunum shows no sign of inflammation. One week post-Nb infection, there are clear signs of oedema and inflammatory cell infiltration in the jejunum. Three weeks post-Nb infection, the time point when experiments were performed, no oedema or inflammatory cell infiltrates are observed in the jejunum.

pH adjusted to 7.3 by using NaOH, and the corresponding intracellular solution was (mM): Hepes 10.0, CsCl 130.0, $MgCl_2$ 1.0, $CaCl_2$ 1.0, EGTA 2.0, K_2ATP 2.0, Na_3GTP 0.2, pH adjusted to 7.25 by using CsOH. All experiments were performed at a temperature of 30–33°C.

Data were analysed by using pClamp 9 software (Axon Instruments). Experiments testing the neuronal excitability were performed in current-clamp mode. Cell recordings were held for $\geq$2 min to allow the resting membrane potential to stabilize prior to current stimulation with a 500 ms current pulse. Current pulses were repeated in 10 pA steps until an AP was elicited. A similar protocol was used in experiments to determine the AP parameters, with the exception that the current duration was 7 ms. A linear leak subtraction protocol in the presence of TTX was used for TTX-R Na^+ current isolation by holding at −100 mV for 100 ms before stepping to a test voltage of between −90 and +20 mV in 10 mV steps. A similar protocol has been used to record TTX-R Na^+ currents in previous studies (Akopian *et al.* 1999).

Real-time quantitative PCR

Immediately after sacrificing CTB-488-labelled mice (see above), DRG from T9–T13 were collected, placed in tissue freezing medium (TFM·, Triangle Biomedical Sciences, Durham, NC, USA), and stored at −80°C. Approximately 150 fluorescently labelled neurons were isolated per animal from 12 μm cryostat sections, by laser capture microdissection using an Axiovert 135 microscope (Zeiss, Göttingen, Germany) equipped with a P.A.L. microbeam (P.A.L. Microlaser Technologies AG, Bernried, Germany). Subsequently, RNA was isolated from the laser-captured samples using RNeasy MinElute Spin Columns (Qiagen, Venlo, Netherlands) and linearly amplified in two rounds. First-strand (Superscript III, Invitrogen, Carlsbad, CA, USA) and second-strand cDNA synthesis (*Bst* polymerase, Epicentre, Madison, WI, USA) was followed by RNA transcription using the AmpliScribe T7 High Yield Transcription Kit (Epicentre). The resulting amplified RNA was incubated with DNAse I and purified using RNeasy MinElute Cleanup Kit (Qiagen). A second round of RNA amplification was performed as described above, except that random hexamer primers were used to prime the reverse-transcription reaction and that the second-strand cDNA reaction was primed with T7 oligonucleotide. Finally, first-strand cDNA synthesis was performed on 50 ng second-round-amplified RNA using random hexamer primers and SuperscriptII RT (Invitrogen).

Real-time quantitative PCR was performed on a ABIPrism 7900 cycler (Applied Biosystems, Foster City, CA, USA) using a Taqman PCR kit (Applied Biosystems). Serial dilutions of cDNA were used to generate standard curves of threshold cycles *versus* the logarithms of concentration for the moderately expressed housekeeping gene ATPSase (Vandesompele *et al.* 2002), $Na_v1.8$ and $Na_v1.9$. Oligonucleotide primers (Eurogentec, Seraing, Belgium) used for ATPSase were 5′-GCA-CTG-CAA-CTG-ATC-TCT-CCA-T-3′ (forward), 5′-GCT-CTT-GTG-TGG-CCT-GCA-T-3′ (reverse), and 5′-Fam-CAA-GCG-AGA-GCT-CAG-GTT-TCC-TTC-Tamra-3′ (probe). The primers used for $Na_v1.8$ were 5′-GAG-GAG-GAT-GGC-GTG-TCA-CT-3′ (forward), 5′-GGA-GCC-CAC-CGT-TGT-CAT-T–3′ (reverse), and 5′-Fam-GCC-ATG-AAT-GTA-ACA-TAG-CCT-TCC-CTG-GG-Tamra-3′ (probe). The primers used for $Na_v1.9$ were 5′-GAA-CAA-GCG-GCG-GAC-TCA-3′ (forward), 5′-GAC-ACC-AAC-CTA-TCA-CCT-CTT-TCA-3′ (reverse), and 5′-Fam-ACA-GGC-CGT-TCA-ACT-TGT-TTT-TT-Tamra-3′ (probe). Data are presented as the relative expression of either $Na_v1.8$ or $Na_v1.9$ *versus* the housekeeping gene ATPSase.

Results

Excitability of DRG neurons from sham and Nb-infected Balb/c mice

Whole-cell voltage-clamp recordings were made from fluorescently labelled DRG neurons from 37 sham and 54 infected cells. These experiments were performed on neurons from 10 sham and 13 infected mice. Sham neurons had a mean capacitance of 23.0 ± 1.3 pF, compared to 21.4 ± 1.2 pF in infected neurons. All cells had a capacitance of < 40 pF, and there was no significant difference between these parameters ($P = 0.32$). In current-clamp mode, the mean resting membrane potential (RMP) was -51.8 ± 1.1 mV in sham and -50.4 ± 0.7 mV in infected DRG neurons ($P = 0.19$). Neurons were injected with a 500 ms pulse in 10 pA increments until an AP was elicited, in order to determine the rheobase. The normalized rheobase of 37 sham neurons was 4.8 ± 1.1 pA pF^{-1}, and the rheobase of 54 infected neurons was 1.8 ± 0.3 pA pF^{-1} ($P = 0.0053$). Cells were then injected with 2× rheobase current, and the number of APs elicited was counted as a measure of neuronal excitability (Fig. 3). The mean number of APs at 2× rheobase was more than doubled in DRG neurons from infected animals (6.8 ± 0.8) compared to sham animals (2.6 ± 0.5) ($P < 0.0001$).

TTX-R currents in DRG neurons from sham and Nb-infected Balb/c mice

Different voltage-ramp protocols were successfully performed on 10 sham and 7 infected neurons in order to assess any changes in TTX-R currents with Nb infection. These experiments were performed on neurons from three

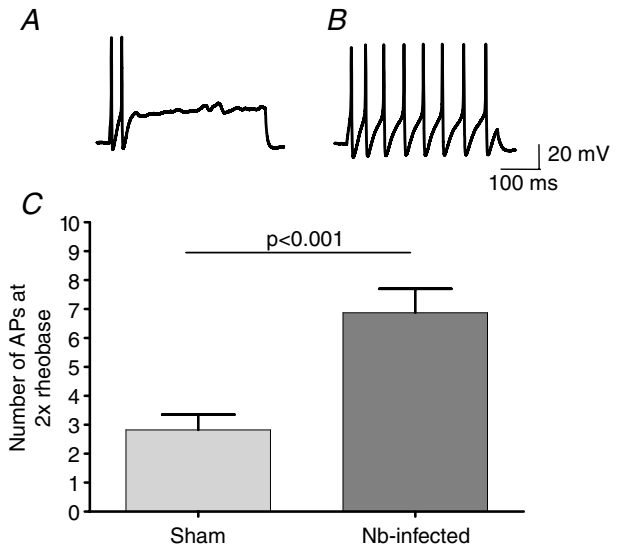

Figure 3. Excitability of DRG neurons in sham *versus* Nb-infected Balb/c mice
A, an example of AP firing elicited by a 500 ms 2× rheobase current pulse in a DRG neuron isolated from a sham Balb/c mouse. *B*, an example of AP firing elicited by a 2× rheobase current pulse in a DRG neuron isolated from an infected Balb/c mouse. *C*, the mean data (± S.E.M.) representing the number of APs induced by a 2× rheobase 500 ms current pulse in sham ($n = 37$) and Nb-infected animals ($n = 54$).

sham and two infected mice. In the presence of 300 nM TTX, cells were held at a −100 mV as a conditioning pulse to evoke total TTX-R currents. The total TTX-R current elicited over the entire voltage scale in these neurons is plotted in Fig. 4. The peak TTX-R current in sham neurons was -47.9 ± 10.4 pA pF^{-1}, whereas the peak TTX-R current in infected neurons was -84.9 ± 11.4 pA pF^{-1} ($P = 0.055$). ANOVA analysis of the entire voltage scale shows that there was a significant increase in TTX-R current in Nb-infected DRG neurons ($P < 0.01$).

Action potential parameters in DRG neurons from $Na_v1.9^{-/-}$ and $Na_v1.8^{-/-}$ mice

The role of $Na_v1.9$ and $Na_v1.8$ currents in AP firing and excitability was assessed by recording from DRG neurons that were isolated from $Na_v1.9^{-/-}$ and $Na_v1.8^{-/-}$ knockout mice, compared to wild-type animals. These experiments were performed on neurons from four sham or infected mice from each of the following four strains; $Na_v1.8^{+/+}$, $Na_v1.8^{-/-}$, $Na_v1.9^{+/+}$ and $Na_v1.9^{-/-}$. For this analysis, a full AP was defined by the following two criteria: (i) the peak of the AP was >+5 mV, and (ii) the amplitude of the AP from threshold to peak was >20 mV. $Na_v1.9^{-/-}$ neurons exhibited similar AP characteristics to those from $Na_v1.9^{+/+}$ mice. However, APs in $Na_v1.8^{-/-}$ neurons were quite different when compared to DRG neurons from $Na_v1.8^{+/+}$ mice. While all $Na_v1.8^{+/+}$ neurons exhibited full APs, only 66% of $Na_v1.8^{-/-}$ neurons exhibited full APs. Furthermore, even when only those $Na_v1.8^{-/-}$ neurons which exhibited full APs were compared to $Na_v1.8^{+/+}$ APs, the peak amplitude reached by APs was significantly lower in $Na_v1.8^{-/-}$ neurons (25 ± 2 mV) than $Na_v1.8^{+/+}$ neurons (42.3 ± 1.5 mV, $P < 0.001$).

Excitability of DRG neurons from $Na_v1.9^{+/+}$ and $Na_v1.9^{-/-}$ mice

Experiments were performed on eight $Na_v1.9^{+/+}$ mice and eight $Na_v1.9^{-/-}$ mice. Patch-clamp recordings were made

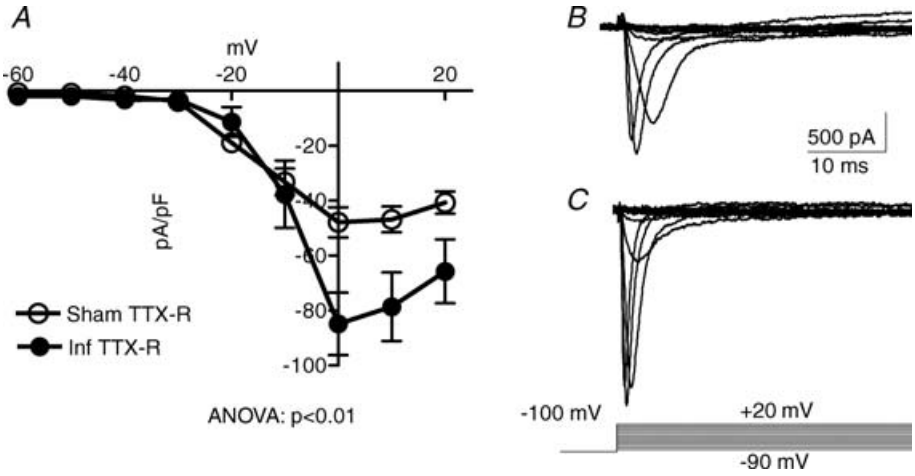

Figure 4. TTX-R currents in Nb-infected neurons
A, current–voltage relationships in DRG neurons from sham ($n = 10$) *versus* Nb-infected ($n = 7$) Balb/c mice recorded in Krebs containing TTX (0.3 μM). A linear leak subtraction protocol was used for TTX-R Na^+ current stimulation by holding at −100 mV for 100 ms before stepping to a test voltage of between −90 and +20 mV in 10 mV steps (mean ± S.E.M.). *B*, an example of the current evoked by the voltage-step protocol in a sham neuron. *C*, an example of the current evoked by the voltage-step protocol in an infected neuron.

Table 1. Summary of the results of the patch-clamp electrophysiological recordings from DRG neurons isolated from sham or Nb-infected $Na_v1.9^{-/-}$ and $Na_v1.9^{+/+}$ mice

	$Na_v1.9^{+/+}$			$Na_v1.9^{-/-}$		
	Sham	Nb-infected	*P* value	Sham	Nb-infected	*P* value
n	20	17		18	18	
Capacitance (pF)	33.1 ± 3.8	26.5 ± 3.0	0.19	29.9 ± 3.3	31.5 ± 3.8	0.75
Resting membrane potential (mV)	−55.3 ± 2.5	−54.2 ± 2.4	0.75	−52.4 ± 1.8	−50.2 ± 2.2	0.4
Rheobase (pA)	129 ± 40	80 ± 17	0.29	119 ± 35	65 ± 21	0.19
Normalized rheobase (pA pF^{-1})	4.3 ± 1.3	3.8 ± 0.9	0.61	3.7 ± 0.8	2.4 ± 0.8	0.28
Number of APs at 2× rheobase	1.9 ± 0.3	3.6 ± 0.7	0.001	1.7 ± 0.4	4.7 ± 0.6	0.001

Data are expressed as mean ± S.E.M.; groups were compared by unpaired *t* tests.

from DRG neurons isolated from $Na_v1.9^{-/-}$ knockout mice and littermate wild-type mice ($Na_v1.9^{+/+}$) that were either sham or Nb-infected (Table 1). Similar data were obtained in neurons from $Na_v1.9^{+/+}$ animals as the data recorded in DRG from Balb/c mice. Neither the mean capacitance nor the RMP was significantly different between neurons from sham and infected $Na_v1.9^{+/+}$ animals. The rheobase in infected neurons was not significantly different from sham animals. The number of APs at 2× rheobase was significantly increased in neurons derived from infected Nav1.9$^{+/+}$ animals when compared to sham (Fig. 5).

Recordings in DRG neurons from $Na_v1.9^{-/-}$ mice were not dramatically different to those obtained from $Na_v1.9^{+/+}$ mice (Table 1). Hence there was no difference between the mean capacitance of sham and infected neurons or between the RMP (Table 1). The mean number of APs at 2× rheobase was significantly increased in infected compared to sham neurons in $Na_v1.9^{-/-}$ mice (Fig. 5).

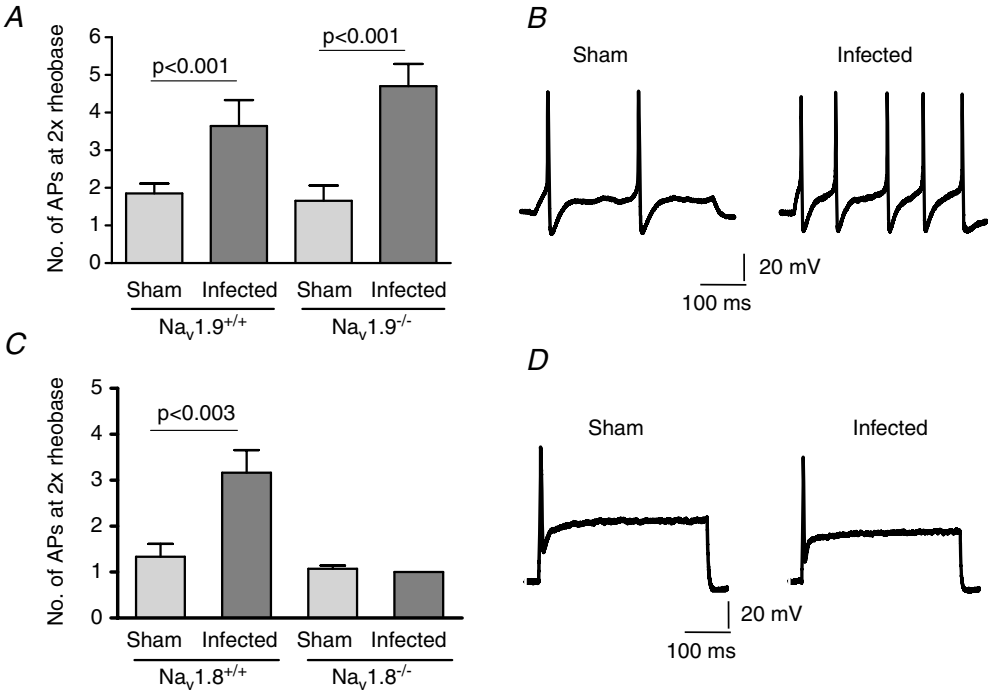

Figure 5. Excitability of DRG neurons in sham and Nb-infected $Na_v1.9^{-/-}$ and $Na_v1.8^{-/-}$ mice and wild-type littermate controls

A, mean data (± S.E.M.) respresenting the number of APs induced by a 2× rheobase 500 ms current pulse in sham ($n = 20$) and Nb-infected ($n = 17$) $Na_v1.9^{+/+}$ neurons, and in sham ($n = 18$) and Nb-infected ($n = 18$) $Na_v1.9^{-/-}$ animals. *B*, an example of AP firing elicited by a 2× rheobase current pulse in sham and infected neurons isolated from a $Na_v1.9^{-/-}$ mouse. *C*, mean data (± S.E.M.) respresenting the number of APs induced by a 2× rheobase current pulse in sham ($n = 18$) and Nb-infected ($n = 19$) $Na_v1.8^{+/+}$ neurons, and in sham ($n = 14$) and Nb-infected ($n = 13$) $Na_v1.8^{-/-}$ animals. *D*, an example of AP firing elicited by a 2× rheobase current pulse in sham and infected neurons isolated from a $Na_v1.8^{-/-}$ mouse.

Table 2. Summary of the results of the patch-clamp electrophysiological recordings from DRG neurons isolated from sham or Nb-infected $Na_v1.8^{-/-}$ and $Na_v1.8^{+/+}$ mice

	$Na_v1.8^{+/+}$			$Na_v1.8^{-/-}$		
	Sham	Nb infected	*P* value	Sham	Nb infected	*P* value
n	18	19		14	13	
Capacitance (pF)	21.3 ± 2.4	21.9 ± 1.4	0.82	23.7 ± 3.3	22.4 ± 3.0	0.77
Resting membrane potential (mV)	−57.6 ± 2.5	−50.7 ± 1.9	0.41	−54.6 ± 1.8	−57.4 ± 2.1	0.22
Rheobase (pA)	180 ± 36	80 ± 24	0.03	165 ± 54	169 ± 39	0.95
Normalized rheobase (pA pF^{-1})	11.1 ± 2.5	3.7 ± 1.2	0.01	8.6 ± 3.5	9.9 ± 2.4	0.76
Number of APs at 2× rheobase	1.3 ± 0.3	3.2 ± 0.5	0.003	1.1 ± 0.1	1.0 ± 0	0.34

Data are expressed as mean ± S.E.M.; groups were compared by unpaired *t* tests.

Excitability of DRG neurons from $Na_v1.8^{+/+}$ and $Na_v1.8^{-/-}$ mice

Experiments were performed on eight $Na_v1.8^{+/+}$ mice and eight $Na_v1.8^{-/-}$ mice. The patch-clamp recordings from DRG neurons isolated from $Na_v1.8^{-/-}$ mice and littermate wild-type mice ($Na_v1.8^{+/+}$) from either sham or Nb-infected animals are summarized in Table 2. Again, the data from $Na_v1.8^{+/+}$ animals resembled the results of the Balb/c mice and the $Na_v1.9^{+/+}$ wild-type animals, with a lower rheobase and a significantly increased number of APs at 2× rheobase in infected compared to sham neurons (Fig. 5). As was recorded in all other cell populations, there was no significant difference following Nb infection in either the mean capacitance or the RMP in $Na_v1.8^{-/-}$ mice (Table 2). However, neither the rheobase of $Na_v1.8^{-/-}$ neurons nor the number of APs fired at 2× rheobase was altered by Nb infection. Interestingly, virtually all $Na_v1.8^{-/-}$ neurons only fired one AP at 2× rheobase, regardless of whether animals were sham or Nb-infected.

mRNA expression of $Na_v1.8$ and $Na_v1.9$ in DRG neurons

As the electrophysiological recordings provide evidence that changes in $Na_v1.8$ but not $Na_v1.9$ currents underlie Nb infection-induced hyperexcitability, $Na_v1.8$ and $Na_v1.9$ mRNA expression in DRG neurons projecting to the gut was assessed by quantitative PCR. The relative expression of either $Na_v1.8$ or $Na_v1.9$ mRNA was not significantly altered in Nb-infected mice compared to sham animals (see Fig. 6).

Discussion

This study is the first to show a prolonged sensory neuron hyperexcitability that persists in the absence of any ongoing inflammation. The increase in excitability of peritoneal DRG neurons following a transient inflammation of the jejunum is due to an increase in TTX-R current that is characteristic of $Na_v1.8$. These data are supported by the fact that DRG neurons from $Na_v1.9^{-/-}$ mice still are hyperexcitable in response to Nb infection, whereas DRG neurons from $Na_v1.8^{-/-}$ mice are less excitable and are not altered by Nb infection.

TTX-R current was upregulated in Nb-infected Balb/c mice. This TTX-R current was activated at approximately −30 mV and hence had properties consistent with $Na_v1.8$. This is the same current that is upregulated acutely in a mouse TNBS-colitis model (Beyak *et al.* 2004). These investigators isolated DRG neurons during the period of acute inflammation that is induced by intracolonic TNBS application (7–10 days post-treatment). Hence the increase of $Na_v1.8$ currents in DRG neurons is presumably a consequence of the TNBS-induced acute colonic inflammation. In the present study, animals were

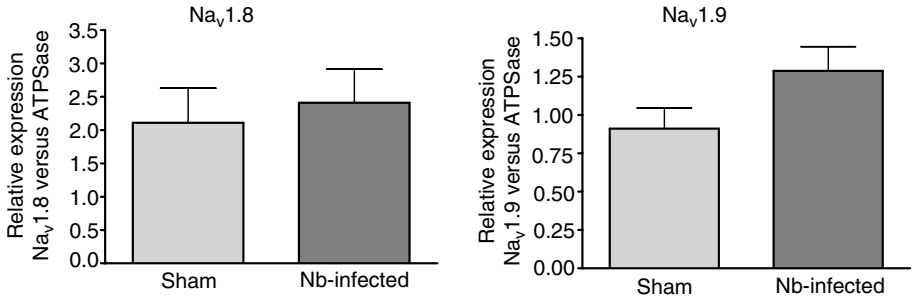

Figure 6. Relative mRNA expression levels of $Na_v1.8$ and $Na_v1.9$ in Nb-infected DRG neurons
Relative mRNA expression level of $Na_v1.8$ in DRG neurons from sham ($n = 8$) and Nb-infected ($n = 7$) Balb/c mice (mean ± S.E.M., $P = 0.69$) on left. On the right is the relative mRNA expression level of $Na_v1.9$ in DRG neurons from sham ($n = 9$) and Nb-infected ($n = 11$) Balb/c mice ($P = 0.09$).

infected with Nb, which is a nematode that produces a mild jejunal inflammation that is resolved after 10 days (Stadnyk *et al.* 1990). In contrast to Beyak *et al.* (2004), we investigated excitability and DRG neuronal function at 20–24 days post-Nb infection and thus not at a time point of acute inflammation. Clearly it would be of interest to determine if $Na_v1.8$ currents are also increased in DRG neurons innervating the jejunum during the acute inflammation induced by Nb infection (3–5 days post-infection), to the same extent as those innervating the colon are increased by TNBS application. Similarly it would be of interest to determine whether $Na_v1.8$ currents are still increased after the inflammation has resolved in the TNBS colitis model.

That the increased TTX-R current is $Na_v1.8$, and that this current drives the altered neuronal excitability in Nb-infected mice is supported by the observation that $Na_v1.8^{-/-}$ mice failed to exhibit any increase in DRG excitability after Nb infection. In contrast, hyperexcitability was evident in $Na_v1.9^{-/-}$ mice similar to that seen in the wild-type and Balb/c mice. In sham $Na_v1.8^{-/-}$ neurons, stimulation at 2× rheobase evoked only one AP, whereas multiple action potentials were generated in sham wild-type and $Na_v1.9^{-/-}$ neurons. Hence it might be argued that the lower baseline excitability in the DRG from uninfected $Na_v1.8^{-/-}$ animals could compromise the ability of these cells to fire multiple action potentials and hence exhibit hyperexcitability, irrespective of the stimulus. This remains a possibility and warrants further investigation. However, in the present study the rheobase was similar in both $Na_v1.8^{-/-}$ and $Na_v1.8^{+/+}$ sham-treated mice, indicating that baseline excitability is not different, but their ability to mount hypersensitivity is. In addition, a previous study (Roza *et al.* 2003) has shown that the ability of nerves to exhibit multiple action potentials after electrical stimulation is not altered in $Na_v1.8^{-/-}$ mice. Interestingly, a recent paper (Matthews *et al.* 2006) has also shown that multiple action potentials can be evoked in dorsal horn neurons in $Na_v1.8^{-/-}$ mice by both thermal and mechanical stimuli, but that it is only the response to mechanical stimuli that is altered in $Na_v1.8^{-/-}$ neurons. Clearly, knocking out $Na_v1.8$ only alters neuronal responses to specific stimuli under specific conditions.

$Na_v1.8$ has been reported to underlie increased neuronal excitability in other studies where there is an ongoing acute insult. In these previously published studies, not only is the insult ongoing, it is also more severe in nature: carrageenan into the hind paw (Tanaka *et al.* 1998), Freunds complete adjuvant into the hind paw (Gould, III *et al.* 2004), capsaicin or mustard oil into the colon (Laird *et al.* 2002), or TNBS into the colon (Beyak *et al.* 2004). The nature of the insult in the present study is much less severe. Nb is a parasitic nematode that produces a mild jejunal inflammation that resolves after 10 days following expulsion of the parasite (Stadnyk *et al.* 1990). Thus at the time of experimentation (days 20–24) there is no ongoing inflammation; this was checked in the present study by histological examination of the small intestine.

Changes in the functional $Na_v1.8$ current recorded in DRG neurons projecting to the gut may be due to alterations in a variety of different parameters that are not mutually exclusive. As these whole-cell electrophysiological recordings capture the total current per cell, an increase in any current may be due to either an increase in the number of channels per cell that contribute to the current, and/or a change in the functional behaviour of the channels. For example, there is evidence that nerve growth factor (NGF) plays a role in regulating $Na_v1.8$ expression levels in DRG neurons (Fjell *et al.* 1999). However, in the present study there was no significant change in $Na_v1.8$ mRNA expression in DRG neurons, suggesting that Nb infection is predominantly altering the functional behaviour of the $Na_v1.8$ channels rather than the number of channels. Significant increases in both mRNA and protein $Na_v1.8$ expression have been reported in somatic inflammation models 4 days after carrageenan hindpaw injection (Black *et al.* 2004). It is impossible to determine why no significant increase in $Na_v1.8$ expression was observed in the present study, as the time course, nature and severity of the insult is quite different.

The complex mechanisms that regulate the $Na_v1.8$ current make it difficult to determine the molecular basis of the altered excitability described in the present study. In addition to the α-subunit, there are at least four different Na_v regulatory β-subunits that associate with Na_v channels either covalently (β_2, β_4) or non-covalently (β_1, β_3). Functional $Na_v1.8$ channels are difficult to transfect into and express in cultured cells (Malik-Hall *et al.* 2003). Nevertheless, coexpression of the α-subunit with different combinations of these β-subunits in *Xenopus* ooctyes yielded functional $Na_v1.8$ channels with different current amplitudes, kinetics and steady-state curves (Vijayaragavan *et al.* 2004). Immunoreactivity for β_1-, β_2- and β_3-subunits is expressed in human sensory neurons, and their expression is altered by nerve injury (Casula *et al.* 2004). In addition a number of other proteins have been identified that may interact with intracellular domains of $Na_v1.8$ (Malik-Hall *et al.* 2003), including linker proteins, enzymes and membrane-associated proteins. It has also been reported that different isoforms of $Na_v1.8$ exist due to alternative splicing of cytoplasmic loop IDII/III (Kerr *et al.* 2004). A change in the expression of any of these parameters has the potential to alter $Na_v1.8$ currents.

No significant differences were observed in any of the parameters measured in DRG neurons from $Na_v1.9^{+/+}$ and $Na_v1.9^{-/-}$ mice and their response to Nb infection, paralleling observations in Balb/c mice. Similarly, there was no significant increase in $Na_v1.9$ mRNA expression. Hence, at least using a Nb infection model, $Na_v1.9$ does

not appear to be involved in any of the functional changes in excitability of DRG neurons. It is well known that the genetic alteration of one particular channel type may lead to an altered expression or function of a related channel, by way of compensation. This has, for example, been demonstrated in $Na_v1.8^{-/-}$ mice that have an upregulation of TTX-S current (Akopian *et al.* 1999). In the present study the relative expression of different sodium channels in $Na_v1.8$ or $Na_v1.9$ knockout mice was not investigated. There are some indications however, that $Na_v1.8$ may be upregulated in $Na_v1.9^{-/-}$ mice. There were more spontaneously active neurons in $Na_v1.9^{-/-}$ compared to $Na_v1.9^{+/+}$ mice (data not shown), and the $Na_v1.8$ peak current was greater in $Na_v1.9^{-/-}$ mice than Balb/c shams (0.95 *versus* 0.74 nA). Thus, it could be speculated that a compensatory increase of $Na_v1.8$ currents in $Na_v1.9^{-/-}$ mice following Nb infection might lead to a further increase in neuronal excitability.

The increase in $Na_v1.8$ following a mild transient inflammation might be clinically relevant, especially as both $Na_v1.8$ and $Na_v1.9$ are expressed in human sensory neurons (Dib-Hajj *et al.* 1999). This raises the potential of these TTX-R currents being potential targets for a variety of pain-related disorders (Lai *et al.* 2004). To this end, a study in a rat model of neuropathic pain has investigated the effects of intrathecal administration of $Na_v1.8$ antisense oligonucleotides. Lai *et al.* (2002) demonstrated that both the expression and the current of $Na_v1.8$ was reduced, and that neuropathic pain induced by spinal nerve injury was reversed without affecting non-noxious sensation or responses to acute pain. There is no ongoing inflammation at the time of the investigations presented here. However, a number of more prolonged post-infectious changes after Nb infection have been reported, including an increase in the number of intestinal mucosal mast cells (IMMCs), the number of nerves in the intestinal mucosa, and the amount of contact between IMMCs and nerve fibres (Stead *et al.* 1987, 1991). It is unclear at this juncture whether these changes have an ongoing influence on the DRG excitability following Nb infection. However, it is of interest to note that a recent study has observed an increase in mast cells in irritable bowel syndrome (IBS) patients, and that this correlates with abdominal pain (Barbara *et al.* 2004), and that alterations in mast cells are responsible for hypersensitivity that underlies IBS (Barbara *et al.* 2006).

The relationship between hypersensitivity observed in whole animals and hyperexcitability in isolated neurons supplying the viscera remains to be elucidated in both this model and others. In the present study, $Na_v1.8^{-/-}$ neurons exhibited a clear-cut lack of hyperexcitability and a decreased ability to form full APs in response to Nb infection. In behavioural testing to algesic stimuli, $Na_v1.8^{-/-}$ mice exhibited analgesia to mechanical stimuli, and minor changes in inflammatory hyperalgesia and thermonociception (Akopian *et al.* 1999). It remains to be determined whether there is a lack of hypersensitivity in $Na_v1.8^{-/-}$ mice following Nb infection.

In summary, the increase in $Na_v1.8$ current that underlies the hyperexcitability following Nb infection may provide an avenue of future research to determine whether long-term changes in $Na_v1.8$ contribute to sensory abnormalities within visceral pathways.

References

Akopian AN, Souslova V, England S, Okuse K, Ogata N, Ure J, Smith A, Kerr BJ, McMahon SB, Boyce S, Hill R, Stanfa LC, Dickenson AH & Wood JN (1999). The tetrodotoxin-resistant sodium channel SNS has a specialized function in pain pathways. *Nat Neurosci* **2**, 541–548.

Anderson CR & Edwards SL (1994). Intraperitoneal injections of Fluorogold reliably labels all sympathetic preganglionic neurons in the rat. *J Neurosci Meth* **53**, 137–141.

Barbara G, Stanghellini V, De Giorgio R & Corinaldesi R (2006). Functional gastrointestinal disorders and mast cells: implications for therapy. *Neurogastroenterol Motil* **18**, 6–17.

Barbara G, Stanghellini V, De Giorgio R, Cremon C, Cottrell GS, Santini D, Pasquinelli G, Morselli-Labate AM, Grady EF, Bunnett NW, Collins SM & Corinaldesi R (2004). Activated mast cells in proximity to colonic nerves correlate with abdominal pain in irritable bowel syndrome. *Gastroenterology* **126**, 693–702.

Beyak MJ, Ramji N, Krol KM, Kawaja MD & Vanner SJ (2004). Two TTX-resistant Na^+ currents in mouse colonic dorsal root ganglia neurons and their role in colitis-induced hyperexcitability. *Am J Physiol Gastrointest Liver Physiol* **287**, G845–G855.

Black JA, Liu S, Tanaka M, Cummins TR & Waxman SG (2004). Changes in the expression of tetrodotoxin-sensitive sodium channels within dorsal root ganglia neurons in inflammatory pain. *Pain* **108**, 237–247.

Casula MA, Facer P, Powell AJ, Kinghorn IJ, Plumpton C, Tate SN, Bountra C, Birch R & Anand P (2004). Expression of the sodium channel beta3 subunit in injured human sensory neurons. *Neuroreport* **15**, 1629–1632.

Coggeshall RE, Tate S & Carlton SM (2004). Differential expression of tetrodotoxin-resistant sodium channels Nav1.8 and Nav1.9 in normal and inflamed rats. *Neuroscience Lett* **355**, 45–48.

Cummins TR, Dib-Hajj SD, Black JA, Akopian AN, Wood JN & Waxman SG (1999). A novel persistent tetrodotoxin-resistant sodium current in SNS-null and wild-type small primary sensory neurons. *J Neuroscience* **19**, 43RC.

Dib-Hajj SD, Tyrrell L, Cummins TR, Black JA, Wood PM & Waxman SG (1999). Two tetrodotoxin-resistant sodium channels in human dorsal root ganglion neurons. *FEBS Lett* **462**, 117–120.

Djouhri L, Fang X, Okuse K, Wood JN, Berry CM & Lawson SN (2003). The TTX-resistant sodium channel Nav1.8 (SNS/PN3): expression and correlation with membrane properties in rat nociceptive primary afferent neurons. *J Physiol* **550**, 739–752.

Fjell J, Cummins TR, Dib-Hajj SD, Fried K, Black JA & Waxman SG (1999). Differential role of GDNF and NGF in the maintenance of two TTX-resistant sodium channels in adult DRG neurons. *Mol Brain Res* **67**, 267–282.

Gould HJ III, England JD, Soignier RD, Nolan P, Minor LD, Liu ZP, Levinson SR & Paul D (2004). Ibuprofen blocks changes in Na v, 1.7 and 1.8 sodium channels associated with complete Freund's adjuvant-induced inflammation in rat. *J Pain* **5**, 270–280.

Herzog RI, Cummins TR & Waxman SG (2001). Persistent TTX-resistant Na^+ current affects resting potential and response to depolarization in simulated spinal sensory neurons. *J Neurophysiol* **86**, 1351–1364.

Kerr NCH, Holmes FE & Wynick D (2004). Novel isoforms of the sodium channels Nav1.8 and Nav1.5 are produced by a conserved mechanism in mouse and rat. *J Biol Chem* **279**, 24826–24833.

Lai J, Gold MS, Kim CS, Bian D, Ossipov MH, Hunter JC & Porreca F (2002). Inhibition of neuropathic pain by decreased expression of the tetrodotoxin-resistant sodium channel, NaV1.8. *Pain* **95**, 143–152.

Lai J, Porreca F, Hunter JC & Gold MS (2004). Voltage-gated sodium channels and hyperalgesia. *Annu Rev Pharmacol Toxicol* **44**, 371–397.

Laird JMA, Souslova V, Wood JN & Cervero F (2002). Deficits in visceral pain and referred hyperalgesia in Nav1.8 (SNS/PN3)-null mice. *J Neurosci* **22**, 8352–8356.

Leong SK & Ling EA (1990). Labelling neurons with fluorescent dyes administered via intravenous, subcutaneous or intraperitoneal route. *J Neurosci Meth* **32**, 15–23.

Linden DR, Sharkey KA, Ho W & Mawe GM (2004). Cyclooxygenase-2 contributes to dysmotility and enhanced excitability of myenteric AH neurones in the inflamed guinea pig distal colon. *J Physiol* **557**, 191–205.

Linden DR, Sharkey KA & Mawe GM (2003). Enhanced excitability of myenteric AH neurones in the inflamed guinea-pig distal colon. *J Physiol* **547**, 589–601.

Mahida YR (2003). Host–parasite interactions in rodent nematode infections. *J Helminthol* **77**, 125–131.

Malik-Hall M, Poon W-YL, Baker MD, Wood JN & Okuse K (2003). Sensory neuron proteins interact with the intracellular domains of sodium channel NaV1.8. *Mol Brain Res* **110**, 298–304.

Matthews EA, Wood JN & Dickenson AH (2006). Nav 1.8-null mice show stimulus-dependent deficits in spinal neuronal activity. *Mol Pain* **2**, 5.

McLean PG, Picard C, Garcia-Villar R, More J, Fioramonti J & Bueno L (1997). Effects of nematode infection on sensitivity to intestinal distension: role of tachykinin NK2 receptors. *Eur J Pharmacol* **337**, 279–282.

Peeters PJ, Aerssens J, de Hoogt R, Stanisz A, Gohlmann HW, Hillsley K, Meulemans A, Grundy D, Stead RH & Coulie B (2006). Molecular profiling of murine sensory neurons in the nodose and dorsal root ganglia labeled from the peritoneal cavity. *Physiol Genomics* **24**, 252–263.

Priest BT, Murphy BA, Lindia JA, Diaz C, Abbadie C, Ritter AM, Liberator P, Iyer LM, Kash SF, Kohler MG, Kaczorowski GJ, MacIntyre DE & Martin WJ (2005). Contribution of the tetrodotoxin-resistant voltage-gated sodium channel NaV1.9 to sensory transmission and nociceptive behavior. *Proc Natl Acad Sci U S A* **102**, 9382–9387.

Renganathan M, Cummins TR, Hormuzdiar WN & Waxman SG (2000). Alpha-SNS produces the slow TTX-resistant sodium current in large cutaneous afferent DRG neurons. *J Neurophysiol* **84**, 710–718.

Renganathan M, Cummins TR & Waxman SG (2001). Contribution of Nav1.8 sodium channels to action potential electrogenesis in DRG neurons. *J Neurophysiol* **86**, 629–640.

Renganathan M, Gelderblom M, Black JA & Waxman SG (2003). Expression of Nav1.8 sodium channels perturbs the firing patterns of cerebellar Purkinje cells. *Brain Res* **959**, 235–242.

Roza C, Laird JMA, Souslova V, Wood JN & Cervero F (2003). The tetrodotoxin-resistant Na+ channel Nav1.8 is essential for the expression of spontaneous activity in damaged sensory axons of mice. *J Physiol* **550**, 921–926.

Rugiero F, Mistry M, Sage D, Black JA, Waxman SG, Crest M, Clerc N, Delmas P & Gola M (2003). Selective expression of a persistent tetrodotoxin-resistant Na^+ current and NaV1.9 subunit in myenteric sensory neurons. *J Neurosci* **23**, 2715–2725.

Rush AM & Waxman SG (2004). PGE2 increases the tetrodotoxin-resistant Nav1.9 sodium current in mouse DRG neurons via G-proteins. *Brain Res* **1023**, 264–271.

Spiller RC (2004). Inflammation as a basis for functional GI disorders. *Best Pract Res Clin Gastroenterol* **18**, 641–661.

Stadnyk AW, McElroy PJ, Gauldie J & Befus AD (1990). Characterization of *Nippostrongylus brasiliensis* infection in different strains of mice. *J Parasitol* **76**, 377–382.

Stead RH, Kosecka-Janiszewska U, Oestreicher AB, Dixon MF & Bienenstock J (1991). Remodeling of B-50 (GAP-43) - and NSE-immunoreactive mucosal nerves in the intestines of rats infected with *Nippostrongylus brasiliensis*. *J Neurosci* **11**, 3809–3821.

Stead RH, Tomioka M, Quinonez G, Simon GT, Felten SY & Bienenstock J (1987). Intestinal mucosal mast cells in normal and nematode-infected rat intestines are in intimate contact with peptidergic nerves. *Proc Natl Acad Sci U S A* **84**, 2975–2979.

Tanaka M, Cummins TR, Ishikawa K, Dib-Hajj SD, Black JA & Waxman SG (1998). SNS Na^+ channel expression increases in dorsal root ganglion neurons in the carrageenan inflammatory pain model. *Neuroreport* **9**, 967–972.

Vandesompele J, De Preter K, Pattyn F, Poppe B, Van Roy N, De Paepe A & Speleman F (2002). Accurate normalization of real-time quantitative RT-PCR data by geometric averaging of multiple internal control genes. *Genome Biol* **3**, RESEARCH0034.

Vijayaragavan K, Powell AJ, Kinghorn IJ & Chahine M (2004). Role of auxiliary [beta]1-, [beta]2-, and [beta]3–subunits and their interaction with Nav1.8 voltage-gated sodium channel*1. *Biochem Biophys Res Comms* **319**, 531–540.

Acknowledgements

The authors would like to acknowledge the assistance of Elaine Fraser, Aaron Hess, Christine McCaul, Jeinifer Whiteley-Osmond and Terri Slade.